EXPERIMENTAL ESTIMATION OF EMPLACEMENT DEPTH OF GRANITIC DIKES FROM THE SØR RONDANE MOUNTAINS, EAST ANTARCTICA

Takanobu Oba[1] and Kazuyuki Shiraishi[2]

[1]*Department of Geoscience, Joetsu University of Education, Joetsu 943-8512*
[2]*National Institute of Polar Research, Kaga 1-chome, Itabashi-ku, Tokyo 173-8515*

Abstract: In order to estimate the depth of emplacement of the granitic dikes intruded into the granulites of the Sør Rondane Mountains, phase relations of the retrograde granulites adjacent to the dikes and the host granulites were experimentally determined in a temperature range of 600 to 900°C, under water pressures of 0.1–0.33 GPa and oxygen fugacities of the FMQ and NNO buffers. The preliminary experimental results indicate that biotite from retrograde granulite is stable at pressures lower than 0.3 GPa. The stability field of biotite in the gneisses suggests that the depth of emplacement of the granitic dikes from the northern central part of the mountains is similar to that of syenites from the southern central part of the mountains (T. Oba and K. Shiraishi; Proc. NIPR Symp. Antarct. Geosci., **8**, 96, 1995)

key words: biotite, melting experiment, granite emplacement, Antarctica, Sør Rondane Mountains

1. Introduction

The Sør Rondane Mountains (71.5°–72.5°S; 22°–28°E) are underlain by Neoproterozoic medium- to high-grade metamorphic rocks together with various early Paleozoic plutonic rocks and minor mafic dikes (Van Autenboer and Loy, 1972; Shiraishi *et al.*, 1991; Shiraishi and Kagami, 1992).

In the northern central part of the mountains, early Paleozoic granite and pegmatite dikes intrude into granulite facies gneisses, resulting in the host gneisses adjacent to the dikes having retrograde mineral assemblages. Since the adjacent zone appears to be bleached into light color in comparison with the dark host granulite facies rocks, we call the phenomenon the "bleached" zone in the field (Figs. 1a, b). The width of the bleached zone depends on the width of granite and pegmatite dikes. The metamorphic host rock adjacent to a narrow vein several centimeters wide formed narrow bleached zones several centimeters wide, whereas granite dikes several meters wide formed bleached zones of several meters wide on both sides of the dike.

In this study we performed a melting experiment to estimate the stability field of biotite in the bleached gneisses and to determine the depth of emplacement of the granite and pegmatite.
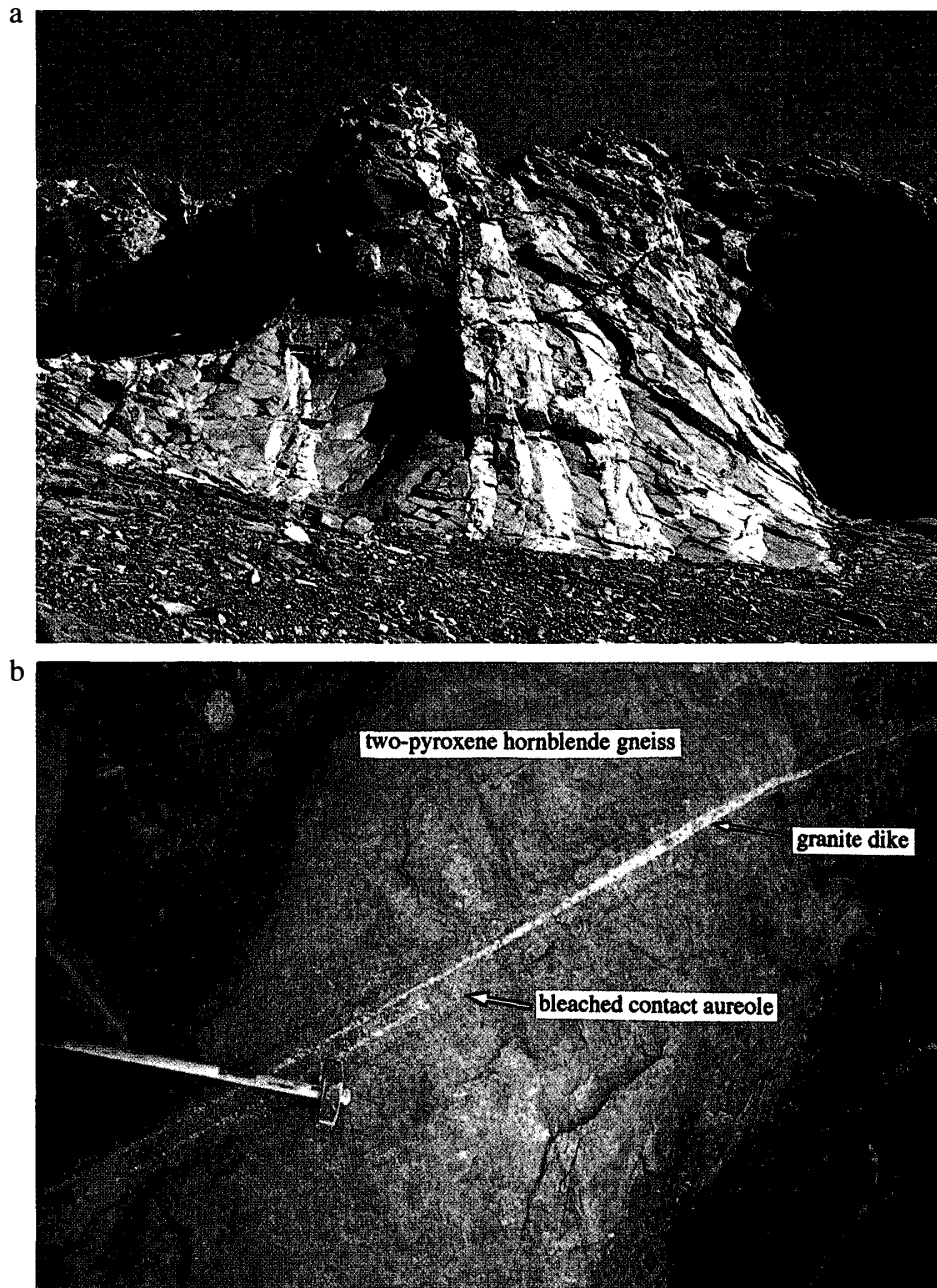
Fig. 1. Photographs of field occurrence of two-pyroxene-bearing hornblende gneisses intruded by granitic dikes, the northwestern part of Brattnipene, the Sør Rondane Mountains.
a. A distant view. Height of the cliff is approximately 150 m.
b. Bleached zone of a few to several cm wide along the granite vein.

2. Petrography and Petrochemistry

The host metamorphic rocks consist mainly of dark brownish felsic two-pyroxene-bearing hornblende gneiss with mafic-rich two-pyroxene-bearing hornblende gneiss layers of several tens of centimeters. The bleached gneisses altered by granite and pegmatite dikes are pale brown to gray biotite-hornblende gneiss.

Nine specimens examined in this study are listed together with the bulk chemical composition and modal composition in Table 1. Four of them are the host two-pyroxene hornblende gneisses (samples 91020404A: 404A, 91020406A: 406A, 91020502A: 502A and 91020502E: 502E), whereas five specimens are retrograde biotite-hornblende gneisses

Table 1.   Chemical and modal compositions of host and bleached gneisses.

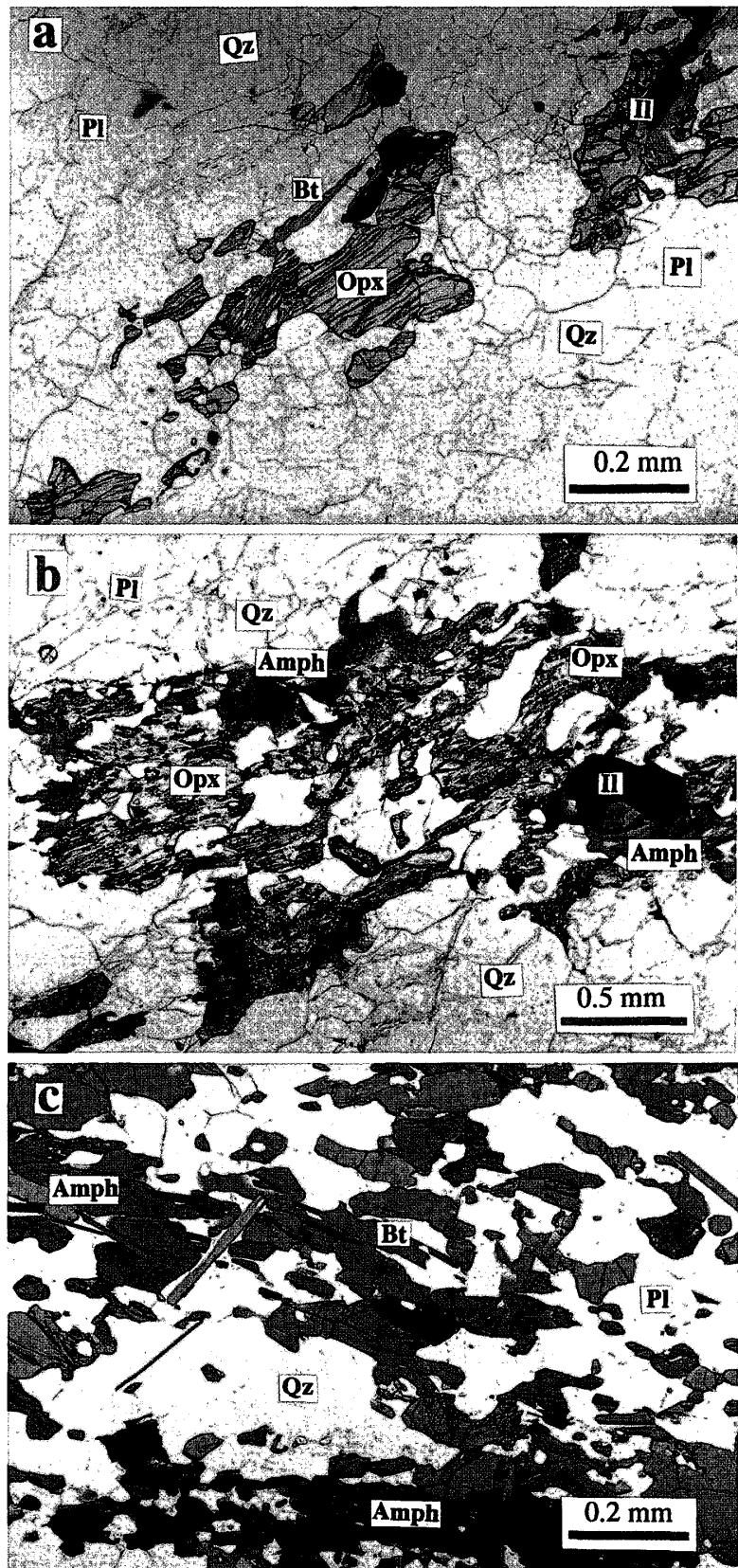|	91020								
	404A	404B	406A	406B	502A	502B	502D	502E	502F
	host	bleached	host	bleached	host	bleached	bleached	host	bleached
Major elements									
SiO2	51.05	50.24	74.70	73.06	71.80	72.24		73.65	74.08
TiO2	0.83	0.83	0.33	0.42	0.38	0.39		0.40	0.35
Al2O3	15.62	15.49	12.86	12.90	13.04	12.61		12.29	12.13
Fe2O3	12.21	12.61	3.33	4.20	5.05	5.36		5.15	4.43
MnO	0.19	0.20	0.04	0.06	0.10	0.10		0.11	0.11
MgO	4.23	4.45	0.34	0.51	0.31	0.34		0.47	0.47
CaO	8.94	9.15	2.65	3.10	2.80	2.73		2.69	2.69
Na2O	3.69	3.56	4.27	4.19	4.57	4.48		4.14	4.06
K2O	1.19	1.13	0.82	0.81	0.82	0.89		0.83	0.86
P2O5	0.12	0.11	0.04	0.05	0.06	0.06		0.07	0.07
Total	98.07	97.77	99.38	99.30	98.93	99.20		99.80	99.25
Trace elements									
Ba	183	104	433	405	421	409		470	453
Co	32	32	16	15	17	17		16	15
Cr	27	24	19	16	13	17		19	15
Cu	11	12	18	17	17	17		18	18
Nb	1	2	5	10	4	5		2	2
Ni	7	2	1	7	7	7		7	5
Rb	4	4	3	15	3	9		2	5
Sr	235	219	180	196	179	165		150	147
V	296	306	41	51	36	36		36	29
Y	15	13	13	23	21	22		20	24
Zn	79	81	21	25	51	48		43	33
Zr	51	47	152	144	150	150		134	133
Modal composition									
Qz	16.2	16.1	71.8	72.2	78.4	72.2	41.1	71.4	
Pl	27.6	29.0	20.6	13.4	9.8	7.5	2.0	11.9	
K-fls	1.6	1.3	0.4	0.4	0.2	0.4	4.5	0.6	
Cpx	3.7	0	2.3	0	1.1	0.1	0	0.2	
Opx	0	0	1.3	tr.	1.7	0	0	0.2	
Hbl	46.6	51.3	1.0	5.7	7.1	10.0	tr.	2.4	
Blue-Hb	0.9	0	0	0	0	0	0	4.5	
Bt	2.5	2.0	1.3	5.7	0.7	8.7	15.5	3.5	
Mus	0	0	0	0	0	0	0.4	3.0	
Gt	0	0	0	0	0	0	36.1	0.0	
Opaq	tr.	tr.	1.2	0.5	0.7	0.8	0.4	2.2	
Others	0.5	0.3	0.2	1.8	0.2	0.2	0.1	0.2	
Total	99.6	100	100.1	99.7	99.9	99.9	100.1	100.1	

Fig. 2. Photomicrographs of the host gneisses.
a. Orthopyroxene partly replaced by biotite and green amphibole in 406A.
b. Orthopyroxene mantled by bluish green hastingsite in 502A.
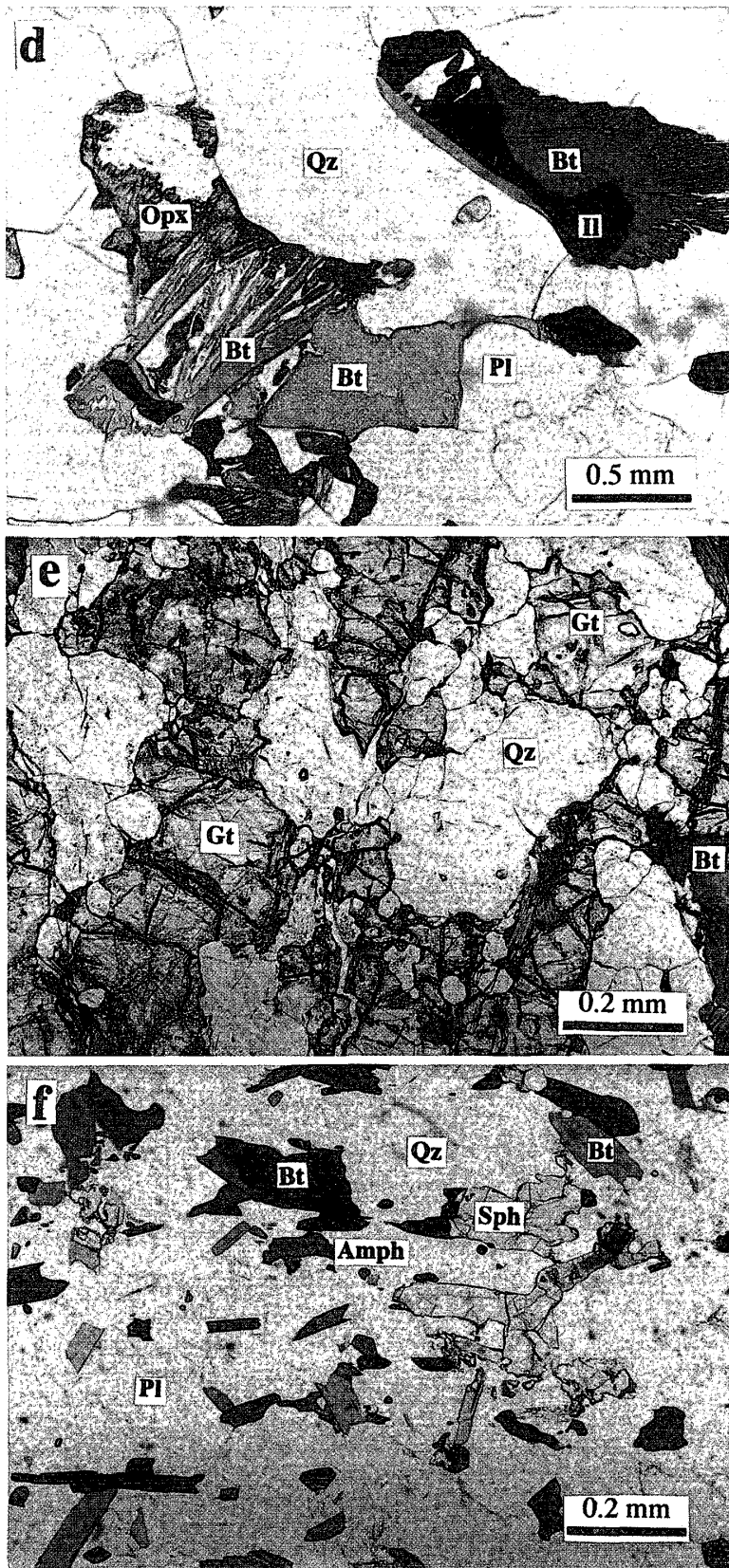*c. Biotite-hornblende gneiss (404B)*

Fig. 2 (continued).

d. Biotite sometimes occurs as the symplectic intergrowth with ilmenite in host gneisses (406B).

e. Garnet occurs along a crack of 502E (502D).

f. Sphene characteristically appears in bleached gneiss (406B).

(samples 91020404B: 404B, 91020406B: 406B, 91020502B: 502B, 91020502D: 502D and 91020502F: 502F) from the bleached zone. The sample numbers indicate the sampling localities, so that the suffix of the sample number, such as A or B, shows the two samples were collected from the same level as a pair of the host and bleached gneisses.

Two-pyroxene hornblende gneisses (host gneisses, hereafter) consist mainly of orthopyroxene, clinopyroxene, quartz and plagioclase, and small amounts of K-feldspar, hornblende, muscovite, ilmenite, apatite and zircon (Fig. 2a). Biotite sometimes occurs as symplectic intergrowths with ilmenite (Fig. 2d). Orthopyroxene is partly replaced by biotite and bluish-green amphibole (Figs. 2a, 2b and 2d).

The biotite hornblende gneisses (bleached gneisses, hereafter) are composed of biotite, amphibole, plagioclase and quartz, and small amounts of K-feldspar, sphene, magnetite, apatite and zircon (Fig. 2c). In contact with the granite dike, all orthopyroxene and clinopyroxene in the host rock were altered to biotite and amphibole. This observation suggests that sufficient water was provided by the granitic dikes during the retro-
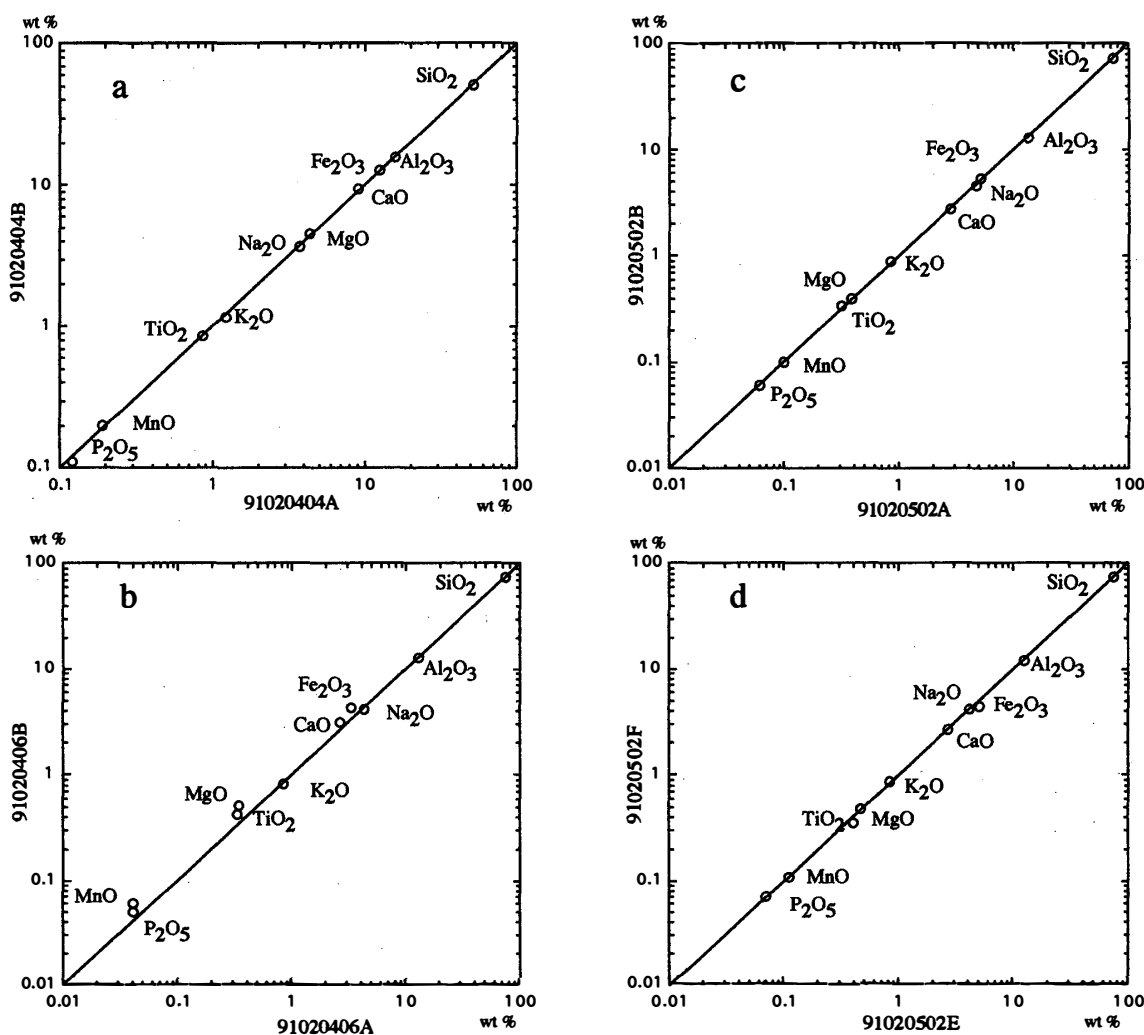

Fig. 3.   Comparison of major element abundance in host gneisses with those in bleached gneisses. a. 404A-404B pair, b. 406A-406B pair, c. 502A-502B pair, d. 502E-502F pair.

gression.   Sometimes, biotite, which occurs together with hornblende, shows a glomeropophyritic texture showing sharp or intertongued grain boundaries.   Modal proportions of orthopyroxene and clinopyroxene decrease, while amphibole and biotite increase (Table 1). Bleached gneisses characteristically contain sphene without ilmenite (Fig. 2f), whereas the host gneisses do not contain sphene but ilmenite as the main Ti-containing phase.   Thus, the assemblage of Amph+Ti-rich Bt+Cpx+Opx+Pl+Qz+K-fls+Il+Mt changes to Amph+Ti-poor Bt+Pl+Qz+K-fls+Mt+Sph by thermal effects associated with dike emplacements.

Garnet occurs only along the small vein of 502D (Fig. 2e). The mineral assemblage in the   vein (502D) is different from that of the host rock 502E, as shown in Table 1. It is evident that the garnet is a reaction product of the host granulite (502E) due to the granite intrusion.

Bulk chemical compositions of the host gneisses and bleached gneisses are given in Table 1. Both major and trace elements were determined by X-ray fluorescence spectrometry (Rigaku S3030 type) at Joetsu University of Education.   The samples 404A and 404B are intermediate and other samples are acidic in compostion. Logarithmic plots of
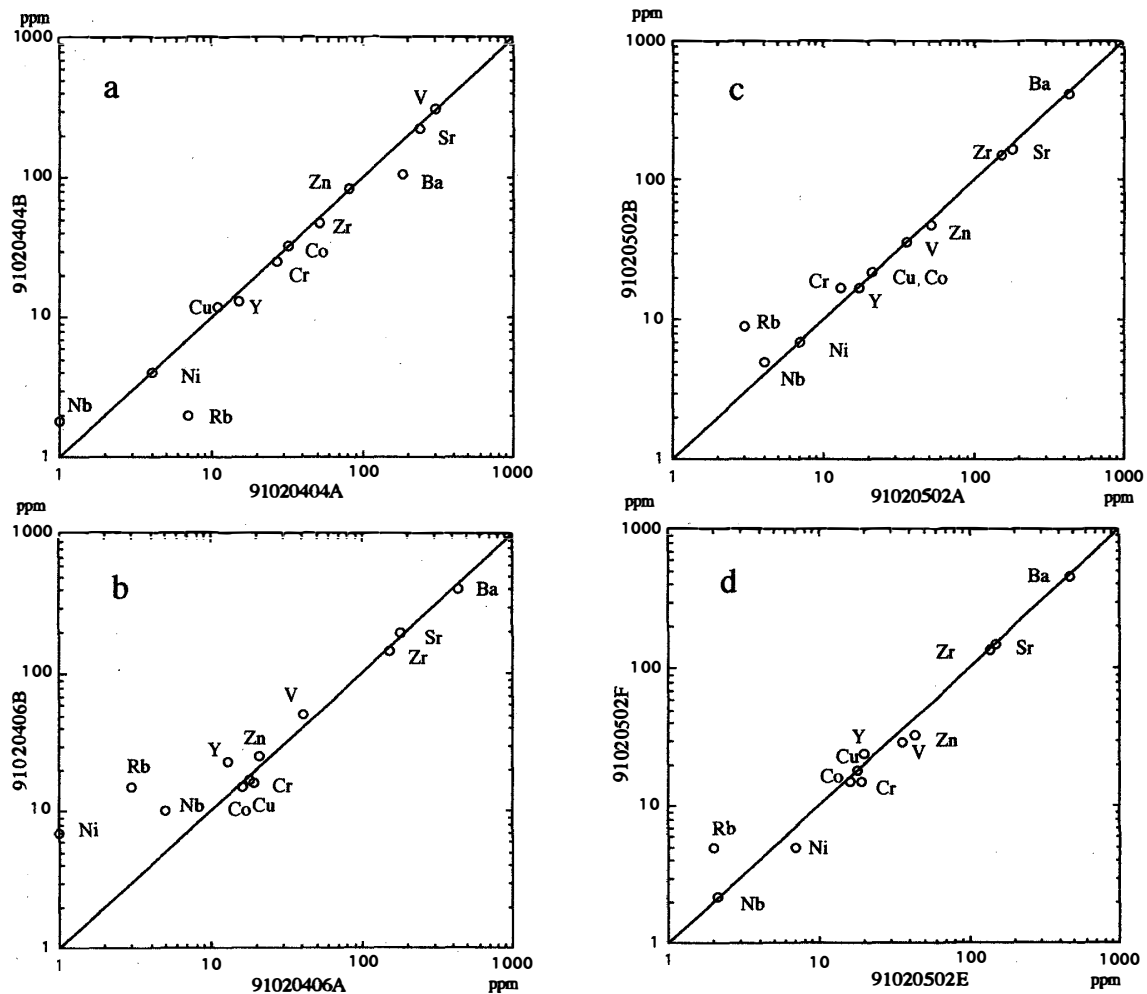

Fig. 4.   Comparison of trace element abundance in host gneisses with those in bleached gneisses.
a. 404A-404B pair, b. 406A-406B pair, c. 502A-502B pair, d. 502E-502F pair.

major and trace element abundance of the host gneisses against those in bleached gneisses are shown in Figs. 3 and 4. The distributions of Nb, Ni and Rb are within analytical error in Figs. 3a–3d. The results suggest that granitic rocks have not greatly affected chemical modification during contact metamorphism.

3. Mineral Chemistry

The chemical compositions of minerals were analyzed with a JEOL 733 Superprobe at the National Institute of Polar Research, and EDS (Link Isis 300) at the Joetsu University of Education. Table 2 gives representative compositions of amphibole, biotite and other silicate minerals.

Orthopyroxene and clinopyroxene are ferrosilite and augite according to MORIMOTO *et al.* (1989), respectively. Orthopyroxene contains around 1 wt% MnO. Plagioclase in both gneisses ranges in composition from An18 to An25. K-feldspar is microcline.

Figure 5 shows the chemical compositions of calcic amphibole in terms of Na+K+Ca at A site *vs.* Al^{IV}. They are plotted on the tie line between tremolite-pargasite join and in a tschermakite-rich field of the tremolite-pargasite join. Amphibole in the bleached gneisses (406B and 502B) is slightly pargasite-rich, in other words silica-poor, as compared to amphibole in the host gneisses (406A and 502A). Amphibole in the host part of the host gneiss (502D) occurs as a mantle of orthopyroxene and also coexists with garnet along a small vein, showing a wide composition range. The bluish green color of amphibole in all rocks suggests that the amphiboles are alkali-rich Ca amphibole with high Fe^{3+} contents. Therefore, we calculated Fe^{3+} contents by using the RECAMP (SPEAR and KIMBALL, 1984). The majority of them are plotted on the hastingsite rich side in the Fe^{3+}-Al^{IV} diagram (Fig. 6). According to the classification of LEAKE *et al.* (1997), these amphiboles are hastingsite to ferropargasite. Amphibole in the bleached gneisses at the contact has higher Fe^{3+} content, compared to amphibole in the country rocks. If we calculate the Fe^{3+} content, the difference of Al^{IV} content between bleached gneisses (406B and 502B) and host gneisses (406A and 502A) is not clear, as shown in Fig. 6. Amphibole in the bleached gneisses (406B and 502B) is rich in Na+K at A site and Fe^{3+}, as compared to amphibole in the host gneisses (406A and 502A). The substitutions $NaAl^{IV}=\square Si^{IV}$ and $Fe^{3+}=Al^{VI}$ are invoked.

Figure 7 shows the compositions of biotite. Mg/(Mg+Fe) ratios of biotite in the 406A and 406B pairs are higher than those of the 502 series (502A, 502B and 502D). Biotite in the bleached gneisses (406B and 502B) is silica-rich and Ti-poor (Fig. 8), as compared to biotite in the host gneisses (406A and 502A). F and Cl contents in biotite were not detected with EDS.

4. Experimental Results

Experiments were performed in standard 'cold seal' pressure vessels in a double capsule configuration under water pressures of 0.1–0.33 GPa and oxygen fugacities of the FMQ and NNO buffers. The phases in the run products were identified with X-ray powder diffraction patterns and an optical microscope. The procedure used in this study is described in detail by OBA and SHIRAISHI (1993). The present experiments were

Table 2. Representative microprobe analyses of constituent minerals.

	406A				406B			502A				502B			502D			
	Bt-1	Amp-5	Opx-5	Pl-17	Bt-1	Amp-7	Pl-42	Bt-7	Amp-2	Opx-7	Pl-18	Bt-15	Amp-7	Pl-17	Bt-52	Amp-50	Opx-51	Gt-53
SiO_2	36.22	40.88	49.67	62.37	35.44	39.10	62.14	32.74	39.54	48.21	63.00	34.23	39.10	62.9	34.32	40.62	51.39	37.31
TiO_2	3.90	1.38	0.12	0.17	1.55	0.82	0.15	4.59	1.18	0.05	0.01	3.42	0.77	0	3.20	1.46	0.14	0.14
Al_2O_3	14.97	11.33	0.53	23.28	16.05	12.23	23.61	15.00	12.19	0.39	23.05	15.04	12.25	23.1	14.83	11.30	0.61	20.59
Cr_2O_3		0	0.01	0.09		0.02	0	0	0.01	0.05	0	0	0	0	0	0	0	0.08
FeO	26.03	23.92	37.92	0.08	22.97	24.44	0.07	26.41	26.14	41.08	0.09	28.42	27.70	0.15	31.19	26.15	35.90	34.66
MnO	0.10	0.46	1.03	0.02	0.54	0.64	0.07	0.65	0.67	2.32	0	0.63	1.05	0.01	0.14	0.43	2.41	3.85
MgO	7.53	6.28	10.98	0.03	8.14	5.50	0.00	4.02	4.05	7.37	0	4.13	3.20	0	3.48	4.56	8.43	0.79
CaO	0.15	11.09	0.82	5.27	0.07	11.18	5.43	0.32	10.87	0.53	4.79	0.04	11.09	4.47	0	10.31	0.49	3.95
Na_2O	0.03	0.62	0.03	8.93	0.04	1.47	8.17	0	1.23	0	8.91	0	1.60	9.06	0.07	1.43	0.07	0
K_2O	9.03	2.04	0	0.33	9.07	1.83	0.44	9.27	1.73	0	0.35	8.9	1.62	0.27	8.48	1.65	0	0.04
Total	97.96	98.00	101.11	100.57	93.87	97.23	100.08	93.00	97.61	100.00	100.20	94.81	98.38	99.9	95.71	97.91	99.44	1
Structural formulae																		
Si	5.541	6.379	1.982	2.758	5.599	6.209	2.756	5.384	6.280	1.993	2.787	5.522	6.232	2.79	5.323	6.402	2.065	3.005
Al^{IV}	2.459	1.621	0.018	1.213	2.401	1.791	1.234	2.616	1.720	0.007	1.202	2.478	1.768	1.21	2.677	1.598		
Al^{VI}	0.241	0.462	0.007		0.588	0.499		0.291	0.561	0.012		0.382	0.533		0.583	0.501	0.029	1.954
Ti	0.449	0.162	0.004		0.184	0.098	0.005	0.568	0.141	0.002		0.415	0.092		0.373	0	0.004	0.009
Cr		0		0.003		0.003	0	0	0.001	0.001		0			0.173	0	0.005
Mg	1.717	1.461	0.653		1.917	1.302	0	0.985	0.959	0.454		0.993	0.760		0.805	1.071	0.505	0.095
Fe	3.330	3.121	1.265	0.004	3.035	3.246	0.003	3.632	3.472	1.420	0.003	3.834	3.692	0.01	4.046	3.446	1.207	2.333
Mn	0.013	0.061	0.035		0.072	0.086	0.002	0.091	0.090	0.081		0.086	0.142	0	0.018	0.057	0.082	0.263
Ca	0.025	1.854	0.035	0.244	0.007	1.902	0.258	0.056	1.850	0.023	0.227	0.007	1.894	0.21	0	1.741	0.021	0.341
Na	0.009	0.188	0.001	0.755	0.012	0.453	0.703	0	0.379	0	0.764	0	0.494	0.78	0.021	0.437	0.005	0
K	1.762	0.406	0	0.020	1.828	0.371	0.025	1.945	0.350	0	0.020	1.832	0.329	0.02	1.678	0.332	0	0.004
Total	15.55	15.715	4.000	4.997	15.643	15.960	4.986	15.57	15.803	3.993	5.003	15.55	15.936	5.01	15.524	15.758	3.918	8.009
Mg/Mg+Fe	0.340	0.319	0.344		0.387	0.286		0.216	0.242			0.206	0.171		0.166	0.248	0.295	
An				24.2			26.2				22.5			21.2				
Ab				74			71.3				75.6			77.3				
Or				1.8			2.5				1.9			1.5				

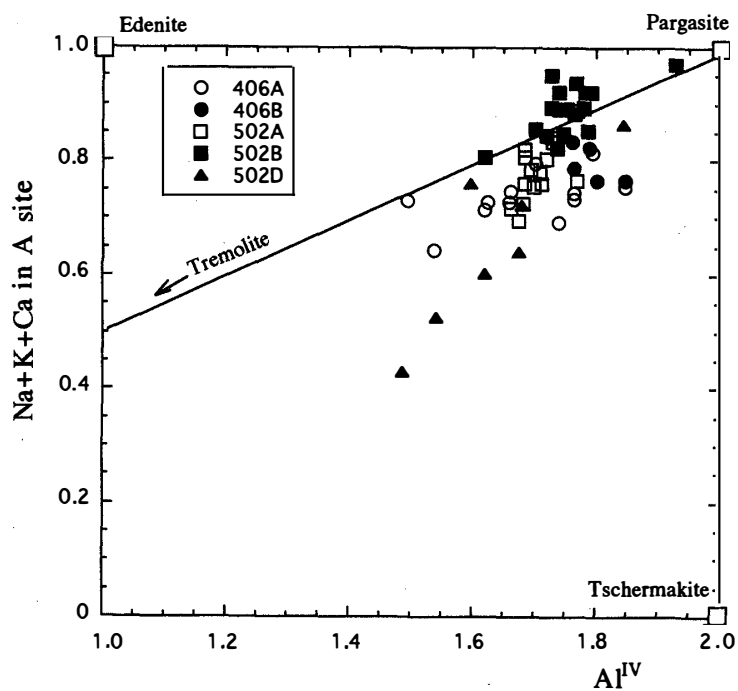Amph: Amphibole, Bt: Biotite, Gt: Garnet, Opx: Orthopyroxene, Pl: Plagioclase

Fig. 5. The chemical variation of Ca-amphibole in gneisses, expressed as the numbers of (Na+K+Ca) in A site vs. Al^{IV} atoms per formula unit.
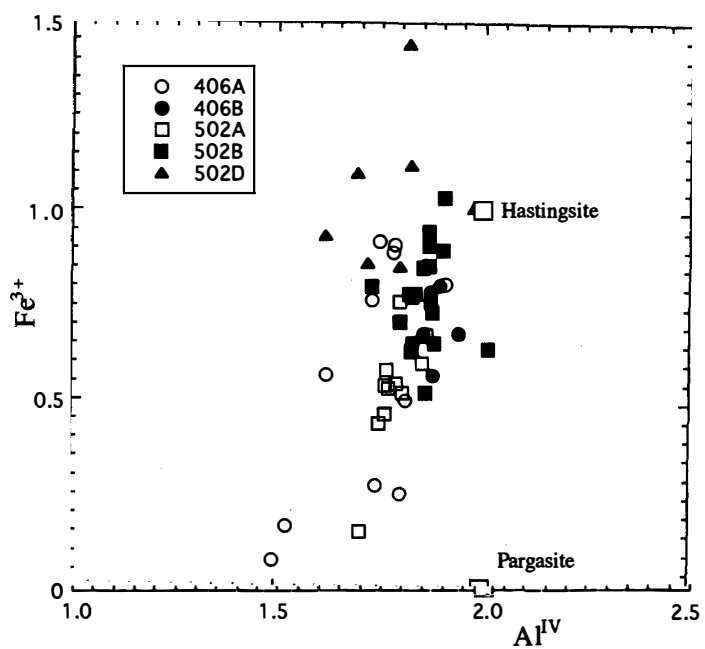

Fig. 6. Plots of Ca-amphibole on a Fe^{3+} vs. Al^{IV} diagram.
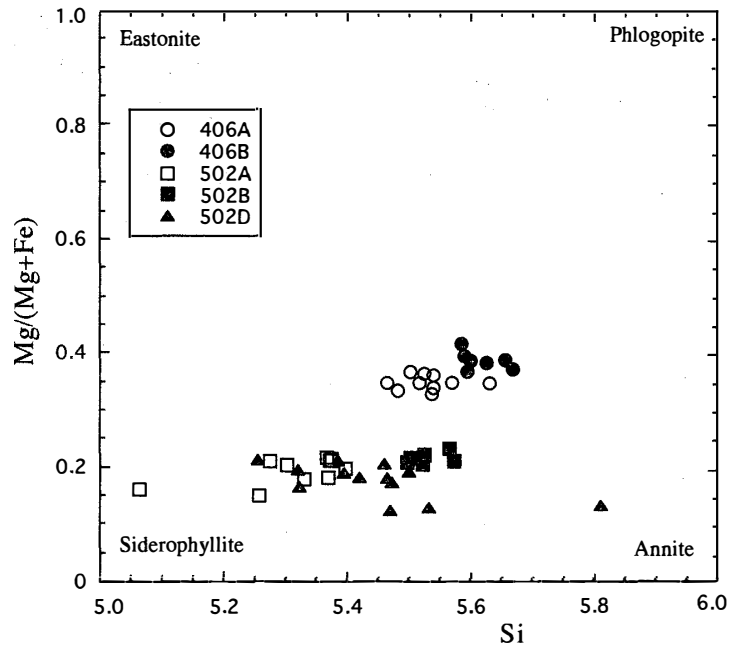
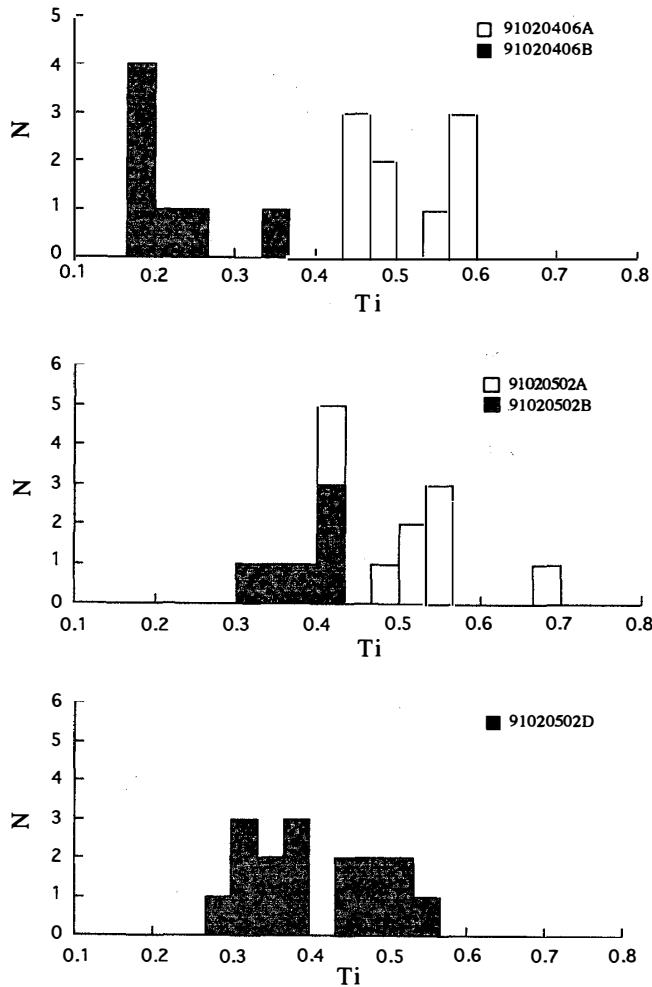*Fig. 7.   Mg/ (Mg+Fe)–Si diagram for biotite.*

Fig. 8.   Frequency of Ti content in biotite from the 406A, 406B, 502A, 502B and 502D. N is the number of samples.

Table 3.   *Experimental results for the four pairs of host and bleached gneisses.*

	Temp. (flC)	Press. (Gpa)	Time (h)	Result
QFM buffer				
406A	775	0.1	682	Amph, Bt, tr.Cpx, Opx, Pl, K-fls, Qz
	800	0.1	382	Amph, Bt, Opx, Pl, Qz, Gl
	840	0.1	252	Amph, Bt, Opx, Pl, Qz, Gl
	875	0.1	194	Opx, Pl, Qz, Gl
	900	0.1	165	Opx, Pl, Qz, Gl
	690	0.2	240	Amph, Bt, Cpx, Opx, Pl, K-fls, Qz
	725	0.2	288	Amph, Opx, Pl, Qz, Gl
	750	0.2	1144	Amph, Opx, Pl, Qz, Gl
	800	0.2	252	Opx, Pl, Qz, Gl
	850	0.2	344	Opx, Pl, Qz, Gl
	900	0.2	165	Opx, Pl, Qz, Gl
	750	0.28	193	Amph, Opx, Pl, Qz, Gl
	720	0.33	120	tr.Amph, Opx, Pl, Qz, Gl
406B	775	0.1	682	Amph, Bt, Pl, K-fls, Qz
	800	0.1	382	Amph, Bt, Opx, Pl, Qz, Gl
	840	0.1	252	Bt, Opx, Pl, Qz, Gl
	875	0.1	194	Bt, Opx, Pl, Qz, Gl
	900	0.1	165	Opx, Pl, Qz, Gl
	690	0.2	240	Amph, Bt, Pl, K-fls, Qz
	725	0.2	288	Amph, Bt, Opx, Pl, Qz, Gl
	750	0.2	1144	Amph, Bt, Opx, Pl, Qz, Gl
	800	0.2	252	Amph, Bt, Opx, Pl, Qz, Gl
	850	0.2	344	Amph, Bt, Opx, Pl, Qz, Gl
	900	0.2	165	Opx, Pl, Qz, Gl
	750	0.28	193	Amph, Bt, Opx, Pl, Qz, Gl
	720	0.33	120	Amph, Bt, Opx, Pl, Qz, Gl
502A	775	0.1	682	Amph, Bt, tr.Cpx, Opx, Pl, K-fls, Qz
	800	0.1	382	Bt, Cpx, Opx, Pl, K-fls, Qz, Gl
	840	0.1	252	Opx, Pl, Qz, Gl
	875	0.1	194	Opx, Pl, Qz, Gl
	900	0.1	165	Opx, Pl, Qz, Gl
	690	0.2	240	Amph, Bt, Cpx, Opx, Pl, K-fls, Qz
	725	0.2	288	Amph, Bt, Cpx, Opx, Pl, Qz, Gl
	750	0.2	1144	Amph, Opx, Pl, Qz, Gl
	800	0.2	252	Amph, Opx, Pl, Qz, Gl
	850	0.2	344	Amph, Opx, Pl, Qz, Gl
	900	0.2	165	Opx, Pl, Qz, Gl
	750	0.28	193	Amph, Opx, Pl, Qz, Gl
	720	0.33	120	Amph, Opx, Pl, Qz, Gl
502B	775	0.1	682	Amph, Bt, Pl, K-fls, Qz
	800	0.1	382	Amph, Bt, Opx, Pl, Qz, Gl
	840	0.1	252	Amph, Opx, Pl, Qz, Gl
	875	0.1	194	Amph, Opx, Pl, Qz, Gl
	900	0.1	165	Opx, Pl, Qz, Gl
	690	0.2	240	Amph, Bt, Pl, K-fls, Qz
	725	0.2	288	Amph, Bt, Opx, Pl, Qz, Gl
	750	0.2	1144	Amph, Opx, Pl, Qz, Gl
	800	0.2	252	Amph, Opx, Pl, Qz, Gl
	850	0.2	344	Amph, Opx, Pl, Qz, Gl
	900	0.2	165	Opx, Pl, Qz, Gl
	750	0.28	193	Amph, Opx, Pl, Qz, Gl
	720	0.33	120	Amph, Opx, Pl, Qz, Gl

Table 3 (continued).

	Temp. (flC)	Press. (Gpa)	Time (h)	Result
NNO buffer				
406A	650	0.1	1262	Amph, Bt, Cpx, Opx, Pl, K-fls, Qz
	690	0.1	762	Amph, Bt, Cpx, Opx, Pl, K-fls, Qz
	700	0.1	762	Amph, Bt, Cpx, Opx, Pl, K-fls, Qz
	750	0.1	762	Amph, Bt, tr.Cpx, Opx, Pl, K-fls, Qz
	775	0.1	393	Bt, Cpx, Opx, Pl, Qz, Gl
	850	0.1	306	Opx, Pl, Qz, Gl
	740	0.15	464	Amph, Bt, Cpx, Opx, Pl, Qz, tr.Gl
	700	0.2	417	Amph, Bt, Cpx, Opx, Pl, K-fls, Qz
	750	0.2	233	Amph, Bt, Cpx, Opx, Pl, Qz, Gl
	800	0.2	207	Amph, Bt, Cpx, Opx, Pl, Qz, Gl
	850	0.2	417	Opx, Pl, Qz, Gl
	750	0.24	191	Amph, Cpx, Opx, Pl, Qz, Gl
406B	650	0.1	1262	Amph, Bt, Pl, K-fls, Qz
	690	0.1	762	Amph, Bt, Pl, K-fls, Qz
	700	0.1	762	Amph, Bt, Pl, K-fls, Qz
	750	0.1	762	Amph, Bt, Pl, K-fls, Qz
	775	0.1	393	Amph, Bt, Opx, Pl, Qz, Gl
	850	0.1	306	Opx, Pl, Qz, Gl
	740	0.15	464	Amph, Bt, Opx, Pl, Qz, Gl
	700	0.2	417	Amph, Bt, Pl, K-fls, Qz
	750	0.2	233	Amph, Bt, Opx, Pl, Qz, Gl
	800	0.2	207	Amph, Opx, Pl, Qz, Gl
	850	0.2	417	Amph, Opx, Pl, Qz, Gl
	750	0.24	191	Amph, Opx, Pl, Qz, Gl
502A	650	0.1	1262	Amph, Bt, Cpx, Opx, Pl, K-fls, Qz
	690	0.1	762	Amph, Bt, Cpx, Opx, Pl, K-fls, Qz
	700	0.1	762	Amph, Bt, Cpx, Opx, Pl, K-fls, Qz
	750	0.1	762	Amph, Bt, tr.Cpx, Opx, Pl, K-fls, Qz
	775	0.1	393	Bt, Opx, Pl, Qz, tr.Gl
	850	0.1	306	Opx, Pl, Qz, Gl
	740	0.15	464	Amph, Bt, Opx, Pl, Qz, Gl
	700	0.2	417	Amph, Bt, Cpx, Opx, Pl, K-fls, Qz
	750	0.2	233	Amph, Opx, Pl, Qz, Gl
	800	0.2	207	Amph, Opx, Pl, Qz, Gl
	850	0.2	417	Opx, Pl, Qz, Gl
	750	0.24	191	Amph, Opx, Pl, Qz, Gl
502B	650	0.1	1262	Amph, Bt, Pl, K-fls, Qz
	690	0.1	762	Amph, Bt, Pl, K-fls, Qz
	700	0.1	762	Amph, Bt, Pl, K-fls, Qz
	750	0.1	762	Amph, Bt, Pl, K-fls, Qz
	775	0.1	393	Amph, Bt, Opx, Pl, Qz, Gl
	850	0.1	306	Opx, Pl, Qz, Gl
	740	0.15	464	Amph, Bt, Opx, Pl, Qz, Gl
	700	0.2	417	Amph, Bt, Pl, K-fls, Qz
	750	0.2	233	Amph, Bt, Opx, Pl, Qz, Gl
	800	0.2	207	Amph, Bt, Opx, Pl, Qz, Gl
	850	0.2	417	Amph, Opx, Pl, Qz, Gl
	750	0.24	191	Amph, Opx, Pl, Qz, Gl

Amph : amphibole, Bt : biotite, Cpx : clinopyroxene, Opx : orthopyroxene,
Pl : plagioclase, K-fls : K-feldspar, Qz : quartz, Gl : glass

carried out under a water saturated condition, assuming that the granitic dike incorporated abundant hydrous fluid.

The experimental results are shown in Table 3 and illustrated in Figs. 9 and 10. The water-saturated solidus temperatures of all samples at FMQ and NNO buffers are 780°C
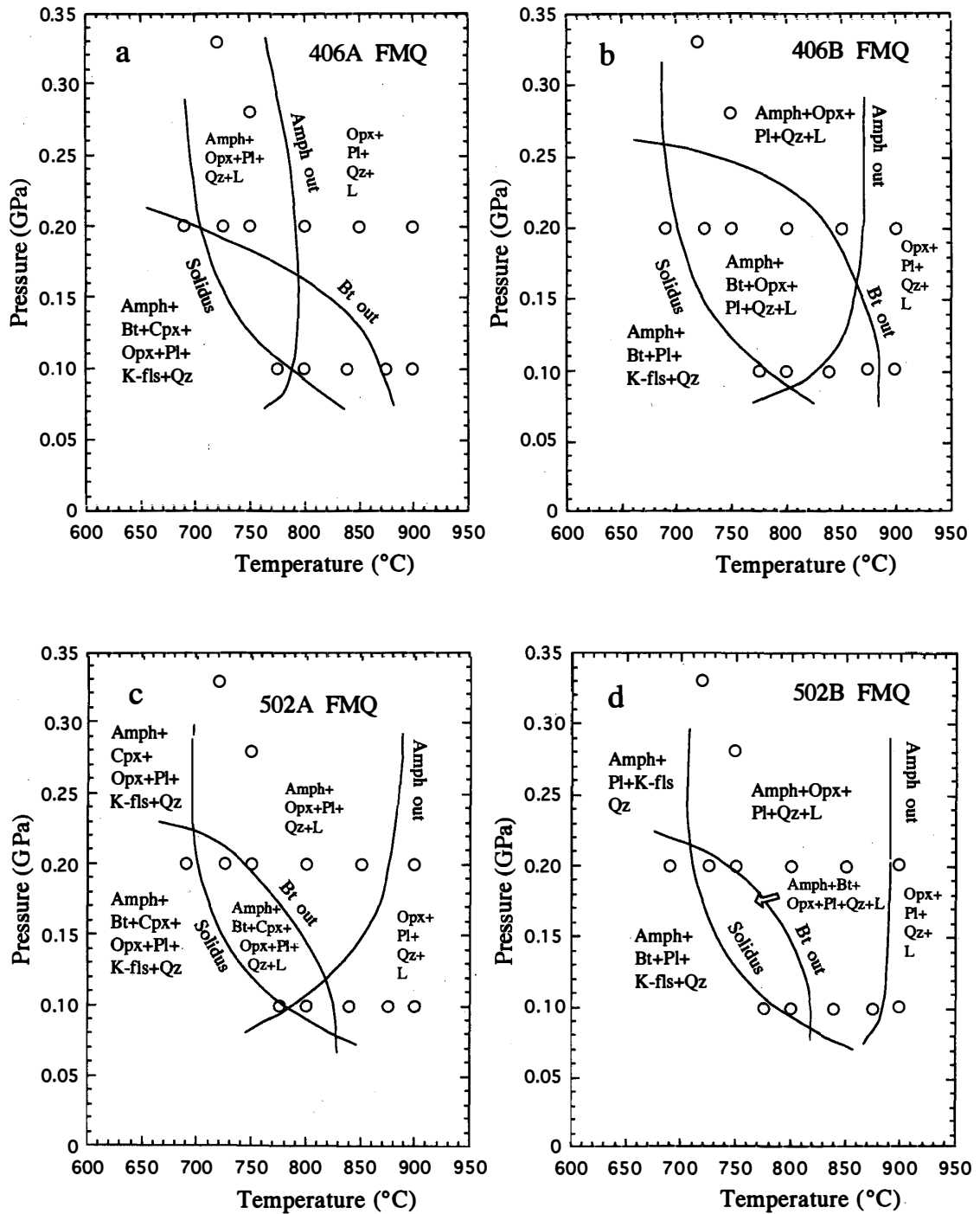

Fig. 9. *P-T diagrams under FMQ buffer. Amph: amphibole, Bt: biotite, Cpx: clinopyroxene, Opx: orthopyroxene, Pl: plagioclase, Qz: quartz, L: liquid (glass) a. 406A, b. 406B, c. 502A, d. 502B.*

at 0.1 GPa and 710°C at 0.2 GPa. The maximum temperature condition of the K-feldspar stability field is located a few degrees above and subparallel to the solidus. Magnetite and vapor are encountered in all run products shown in Figs. 7 and 8. Ilmenite appears in the run product of the 406A and 502A.

The upper temperature stability limit of amphiboles in the 406B and 502B is higher

Fig. 10.   P-T diagrams under NNO buffer. Abbreviations are the same as in Fig. 9.
a. 406A, b. 406B, c. 502A, d. 502B.

than those in the 406A and 502A under both FMQ and NNO buffers. Amphibole is stable at 720°C and 0.33 GPa in the present experiments. We could not determine the upper pressure stability limit of amphibole in all gneisses in the present experiment. In contrast, the biotite stability fields were determined in this experiment. The stability fields of biotite in the runs with 406A (Fig. 9a), 502A (Fig. 9c) and 502B (Fig. 9d) at FMQ buffer, and 502A (Fig. 10c) at NNO buffer, are narrower than those from 406A (Fig. 10a), 406B (Fig. 10b) and 502B (Fig. 10d) at NNO buffer, and 406B (Fig. 9b) at FMQ buffer. The upper pressure stability limit of biotite is not over 0.3 GPa at 600°C regardless of bulk composition or fo_2.

5. Discussion

SHIRAISHI and KOJIMA (1987) estimated, on the basis of geothermo-barometries, that P-T conditions of peak metamorphism in the northern part of the Sør Rondane Mountains are around 800°C and 0.7–0.85 GPa. One of the bleached gneisses, 502D, contains a garnet-biotite assemblage that is useful for temperature estimation. The biotite in this sample has a wide range of Si and Ti contents. Biotite in the host gneisses (406A and 502A) is rich in Ti, as compared to biotite in bleached gneisses (406B and 502B), as shown in Fig. 8. The biotite with the high Ti content may remain as a relic at the stage of host gneiss. Therefore, we calculate the temperature by using biotite with lower Ti content of less than 0.4. Seven selected pairs of biotite and garnet rim adjacent to biotite show equilibrium temperatures at 0.3 GPa between 540 and 610°C by THOMPSON's (1976) thermometer, between 510 and 640°C by FERRY and SPEAR's (1978) thermometer, between 520 and 620°C by HOLDWAY and LEE's (1977) thermometer, and between 550 and 630°C by PERCHUK and LAVRENT'EVA's (1983) thermometer. The solidus temperatures in the present experiments are 780°C at 0.1 GPa and 710°C at 0.2 GPa. These estimated temperatures are below the solidus temperatures. The bleached gneiss characteristically contains magnetite ($Mt_{99}Usp_1$–$Mt_{96}Usp_4$) without ilmenite, whereas the host gneiss contains both ilmenite ($Il_{98}Hem_2$–$Il_{95}Hem_5$) and magnetite ($Mt_{90}Usp_{10}$–$Mt_{88}Usp_{12}$). The compositions of iron-titan oxides suggest that the oxygen fugacity of the bleached gneiss at 600°C was higher than that of the host gneiss at the peak metamorphic condition, according to BUDDINGTON and LINDSLEY (1964).

The present experiment indicates that the upper pressure stability limits of Ti-poor biotite in the gneisses are lower than 0.3 GPa in a temperature range of 600 to 900°C at FMQ and NNO buffers. OBA and SHIRAISHI (1995) reported that the pressure stability limit of amphiboles in two syenites and a granite from Lunckeryggen of the Sør Rondane Mountains are lower than 0.35 GPa. The present and previous experimental results (OBA and SHIRAISHI, 1995) suggest that the depth of emplacement of the intrusive rocks in the Lunckeryggen-Brattnipene region is shallower than 12 km (0.3 GPa).

Acknowledgments

References

Buddington, A.F. and Lindsley, D.H. (1964): Iron-titanium oxide minerals and synthetic equivalents. J. Petrol., **5**, 310–357.

Ferry, J.M. and Spear, F.S. (1978): Experimental calibration of the partitioning of Fe and Mg between biotite and garnet. Contrib. Mineral. Petrol., **66**, 113–117.

Holdway, M.J. and Lee, S.M. (1977): Fe-Mg cordierite stability in high-grade pelitic rocks based on experimental, theoretical and natural observations. Contrib. Mineral. Petrol., **63**, 175–198.

Leake, B.E., Woolley, A.R., Arps, C.E.S., Birch, W.D., Gilbert, M.C., Grice, J.D., Hawthorne, F.C., Kato, A., Kisch, H.J., Krivovichev, V.G., Linthout, K., Laird, J., Mandarino, J.A., Maresch, W.V., Nickel, E.H., Rock, N.M.S., Schumacher, J.C., Smith, D.C. Stephenson, N.C.N., Ungretti, L., Whittaker, E.J.W. and Youzhi, G. (1997): Nomenclature of amphiboles: Report of the subcommittee on amphiboles of the International Mineralogical Association commission on new minerals and mineral names. Am. Mineral., **82**, 1019–1037.

Morimoto, N., Fabries, J., Ferguson, A.K., Ginzburg, J.V., Ross, M., Seifert, F.A., Zussman, J., Aoki, K. and Gottardi, G. (1989): Nomenclature of pyroxenes. Subcommittee on pyroxenes. Commission on new mineral and mineral names (CNMMN). International Mineralogical Association (IMA). Mineral. J., **14**, 198–221.

Oba, T. and Shiraishi, K. (1993): Experimental studies on syenitic rocks in the Yamato Mountains, East Antarctica. Proc. NIPR Symp. Antarct. Geosci., **6**, 72–82.

Oba, T. and Shiraishi, K. (1995): The stability field of amphibole from the Sør Rondane Mountains, East Antarctica: Implication for the emplacement pressure of syenite magma. Proc. NIPR Symp. Antarct. Geosci., **8**, 98–106.

Perchuk, L.L. and Lavrent'eva, I.V. (1983): Experimental investigation of exchange equilibria in the system cordierite-garnet-biotite. Kinetics and Equilibrium in Mineral Reactions, ed. by S.K. Saxena. New York, Springer-Verlag, 199–239.

Shiraishi, K. and Kagami, H. (1992): Sm-Nd and Rb-Sr ages of metamorphic rocks from the Sør Rondane Mountains, East Antarctica. Recent Progress in Antarctic Earth Science, ed. by Y. Yoshida et al. Tokyo, Terra Sci. Publ., 29–35.

Shiraishi, K. and Kojima, S. (1987): Basic and intermediate gneisses from the western part of the Sør Rondane Mountains, East Antarctica. Proc. NIPR Symp. Antarct. Geosci., **1**, 129–149.

Shiraishi, K., Asami, M., Ishizuka, H., Kojima, S., Osanai, Y., Sakiyama, T., Takahashi, Y., Yamazaki, M. and Yoshikura, S. (1991): Geology and metamorphism of the Sør Rondane Mountains, East Antarctica. Geological Evolution of Antarctica, ed. by M.R.A. Thomson et al. Cambridge, Cambridge Univ. Press, 77–82.

Spear, F.S. and Kimball, K.L. (1984): RECAMP—A FORTRAN IV program for estimating Fe^{3+} contents in amphiboles. Computers Geosci., **10**, 317–325.

Thompson, A.B. (1976): Mineral reactions in pelitic rocks; II. Calculation of some *P-T-X* (Fe-Mg) phase relations. Am. J. Sci., **276**, 425–454.

Van Autenboer, T. and Loy, W. (1972): Recent geological investigations in the Sør Rondane Mountains, Belgicafjella and, Sverdrupfjella, Dronning Maud Land. Antarctic Geology and Geophysics, ed. by R.J. Adie. Oslo, Universitetsforlaget, 563–571.